



Cite this: *Chem. Commun.*, 2019, 55, 2880

Received 5th December 2018,  
Accepted 4th February 2019

DOI: 10.1039/c8cc09672d

[rsc.li/chemcomm](http://rsc.li/chemcomm)

## Environmentally responsive photonic polymers

Ellen P. A. van Heeswijk,<sup>†ab</sup> Augustinus J. J. Kragt,<sup>†ab</sup> Nadia Grossiord<sup>id</sup>\*<sup>c</sup> and Albertus P. H. J. Schenning<sup>id</sup>\*<sup>abd</sup>

Stimulus-responsive photonic polymer materials that change their reflection colour as function of environmental stimuli such as temperature, humidity and light, are attractive for various applications (e.g. sensors, smart windows and communication). Polymers provide low density, tunable and patternable materials. This feature article focusses on various autonomously responding photonic polymer materials such as hydrogels, block copolymers and liquid crystals and discusses their potential industrial implementation.

### Introduction

All living organisms show irritability and adaptation, meaning that they have the ability to respond to environmental changes such as temperature, humidity and light. For instance, mammalian

skin adapts to external temperature fluctuations aiding in a process called homeostasis in order to maintain internal body temperature and to function properly.<sup>1</sup> Other organisms use colour changes for camouflage and communication.<sup>2–4</sup> For example, the blue damselfish *Chrysiptera cyanea*, which changes from blue-green at daytime to violet at night in response to light and various beetles, which change their colouration in response to humidity.<sup>5–7</sup> These environmentally responsive systems found in nature have inspired scientists to fabricate artificial self-regulating, adaptive systems for sensors, energy saving, rewritable paper and security features.<sup>8–16</sup>

Environmentally triggered colour changes may arise from modulations of photonic structures. These structures, also called photonic crystals (PCs), consist of 1, 2 or 3 dimensional periodically nano-structured materials with different refractive indices (Fig. 1). This periodic modulation of refractive index

<sup>a</sup> *Stimuli-responsive Functional Materials and Devices, Department of Chemical Engineering, Eindhoven University of Technology, P.O. Box 513, 5600 MB Eindhoven, The Netherlands. E-mail: A.P.H.J.Schenning@tue.nl*

<sup>b</sup> *SCNU-TUE Joint Laboratory of Device Integrated Responsive Materials (DIRM), Guangzhou Higher Education Mega Center, South China Normal University, 510006 Guangzhou, China*

<sup>c</sup> *SABIC, T&I, Plasticslaan 1, 4612 PX Bergen op Zoom, The Netherlands. E-mail: nadia.grossiord@sabic.com*

<sup>d</sup> *Institute for Complex Molecular Systems, Eindhoven University of Technology, P.O. Box 513, 5600 MB Eindhoven, The Netherlands*

<sup>†</sup> E. P. A. van Heeswijk and A. J. J. Kragt contributed equally to this work.



**Ellen P. A. van Heeswijk**

*Ellen van Heeswijk received her Master's degree in Chemical Engineering in 2015 at the Eindhoven, University of Technology in the Netherlands. Afterwards, she joined the group of 'Stimuli-responsive Functional Materials and Devices' at the same University for her PhD studies. She is currently working on stimuli-responsive photonic coatings for plastic substrates based on cholesteric liquid crystals, under supervision of Prof. Dr Albert Schenning and in close collaboration with industry (SABIC).*



**Augustinus J. J. Kragt**

*Stijn Kragt followed the Physical Chemistry Master's programme at the Radboud University Nijmegen, in which he studied liquid crystals and polymer materials supervised by Dr Paul Kouwer. He received his Chemistry Master's degree in 2015. Afterwards, he started his PhD studies at the research group of 'Stimuli-responsive Functional Materials and Devices' at the Eindhoven University of Technology. Here, he is working on responsive photonic coatings based on semi-interpenetrating polymer networks under supervision of Prof. Dr Albert Schenning and in close collaboration with SCNU-TUE Joint Laboratory of Device Integrated Responsive Materials.*



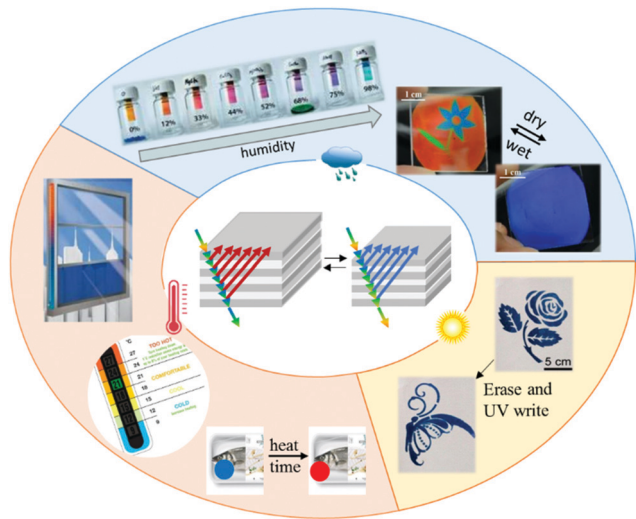


**Fig. 1** Schematic representation of the structure and applications of environmentally responsive photonic polymers. Applications of responsive photonic polymers: (red, temperature as stimulus) thermometer strips, time-temperature integrator and smart energy saving windows. Adapted from ref. 19 and 20; (blue, humidity as stimulus) humidity sensors and rewritable paper using water or exhaled breath as ink. Adapted with permission from ref. 21 (Copyright 2018 ACS publications) and ref. 22 (Copyright 2015 ACS publications). (Yellow, light as stimulus) rewritable paper (outer circle). Adapted with permission from ref. 23. Copyright 2016 ACS publications. Schematic representation of a responsive photonic material e.g. 1D-Bragg reflector (middle).

results in constructive interference of the light reflected at each boundary of refractive index change according to Bragg's law. As such, a photonic structure reflects light of a specific wavelength and may therefore give rise to the appearance of a structural colour. The wavelength that the PC reflects depends

on the refractive indices and periodicity of the materials within a structure. A responsive PC structure can thus be fabricated using materials that change their refractive index or periodicity upon exposure to a stimulus. In case a disappearance of the reflectivity is desired, refractive index matching or a collapse of the internal periodic structure is needed.<sup>5,10,12–14</sup>

Inorganic materials have been used for the fabrication of responsive PC coatings. They have a wide refractive index range, can be processed on large scale with uniform thickness control, switch in the order of nanoseconds and are mechanically stable.<sup>5,8,17,18</sup> However, their response is typically limited to 100 nm shifts at the most, since they rely on minor refractive index changes.<sup>8,18</sup>

In contrast to inorganic materials, polymeric materials can change both refractive index and periodicity of the photonic structures upon exposure to a stimulus. Furthermore, the properties of polymeric materials can be tuned in a modular fashion, are compatible with existing coating and printing methods, can be processed at lower temperatures and possess lower densities compared to inorganic materials.<sup>24,25</sup>

To fabricate environmentally responsive photonic polymers, extensive research on polymer systems that can change volume, refractive index and/or undergo a phase transition upon temperature, humidity or light fluctuations is on-going. Various polymeric systems have been found to have such a response to environmental stimuli, including hydrogels, shape memory polymers and liquid crystal polymers.<sup>5,8,26–29</sup> This feature article focuses on recent developments in the field of photonic polymers that change colouration due to changes in the environmental stimuli: temperature, humidity and light. Other types of stimuli such as electric<sup>30</sup> and magnetic fields<sup>31,32</sup> and chemicals<sup>33</sup> are beyond the scope of this feature article. One-way (irreversible) memory polymers and two-way (reversible)



**Nadia Grossiord**

group of Prof. Stefan Bon dealing with Pickering emulsions at the Warwick University (UK), she worked three years at the Holst Centre (NL) on flexible electronics and printing. Since 2012, she is working in the R&D division of SABIC (NL) in the fields of functional surfaces, liquid crystal polymers and high performance films.

*Nadia Grossiord graduated in 2003 with a Master Degree of Science at the École Européenne de Chimie, Polymères et Matériaux (ECPM) of the Strasbourg University (France) and obtained her PhD from the Eindhoven University of Technology (TU/e) in 2007, working on electrically conductive carbon nanotube-polymer nanocomposites prepared by latex technology, under the supervision of Prof. Cor Koning. After a Post Doc in the*



**Albertus P. H. J. Schenning**

group of Prof. Bert Meijer at Eindhoven University of Technology (TU/e), working on dendrimers. In 1997, he investigated pi-conjugated oligomers and polymers based on triacetylenes with Prof. François Diederich at the ETH in Zurich. From 1998 until 2003, Schenning was a fellow of the Royal Netherlands Academy of Arts and Sciences (KNAW) at the TU/e, active in the field of supramolecular organization of pi-conjugated systems. Currently he leads the research group stimuli-responsive functional materials and devices at the TU/e.

*Albert Schenning studied chemistry at Radboud University Nijmegen, where he obtained his doctorate in 1996. His PhD thesis on supramolecular architectures based on porphyrin and receptor molecules was supervised by Dr Martin Feiters and Prof. Roeland Nolte. In 1996, Schenning was a post-doctoral fellow in the group of Prof. Bert Meijer at Eindhoven University of Technology (TU/e), working on dendrimers. In 1997,*



changing polymer films are the main focus of this feature article. Particular attention is given to the possible scalability and applications of these adaptive soft photonic materials.

## Temperature responsive photonic polymers

Irreversible as well as reversible temperature responsive photonic polymers can be prepared by various methods. By embossing, temperature responsive shape-memory coatings can be prepared showing only one-way responsive behaviour. Reversibly responsive coatings can be achieved by using hydrogel polymers of which the swelling strongly depends on the temperature or cholesteric liquid crystal elastomers or droplets that reversibly reorganize upon temperature fluctuations.

### One-way temperature responsive photonic polymers

Shape memory polymers are attractive to prepare one-way, irreversible temperature responsive photonic materials. Shape memory polymers can fix a temporary shape and recover to their original shape upon heating. For instance, 3D inverse opal structured glassy polymers, such as polyurethane-*co*-tripropylene glycol diacrylate, can be embossed above the glass transition temperature ( $T_g$ , 86 °C) and cooled below the  $T_g$  to freeze in a temporary, non-coloured disordered state. Upon heating above the  $T_g$ , the original shape and photonic structure recovers in approximately 200 s, resulting in a colourless to coloured transition.<sup>34</sup>

A similar effect can be obtained using glassy cholesteric liquid crystal network (LCN) polymers. In cholesteric liquid crystals (CLCs) a periodic refractive index modulation is caused by the helical organization of the liquid crystals. The helical periodicity and thus the reflective wavelength is induced and controlled by a so-called chiral dopant. By embossing a cholesteric LCN above  $T_g$  (ranging from 40 to 60 °C) and subsequently cooling, the cholesteric pitch was compressed, resulting in a blue shift from 580 to 550 nm. Upon subsequent heating above the  $T_g$  the cholesteric pitch restores to its original size in the order of minutes, resulting in a red shift. These materials may be of interest as time-temperature integrators to monitor the cold chain of food and pharmaceuticals as the colour change is irreversible.<sup>35</sup> By fabricating a semi-interpenetrating cholesteric LCN coating the glass transition temperature can be broadened (*i.e.* ranging from 10 to 54 °C). After embossing, these films display multiple highly stable colours within the  $T_g$  range. The relaxation behavior of the embossed film can be mathematically described revealing that, for example, complete recovery of the color when stored at 20 °C is estimated to take more than 30 million years (Fig. 2).<sup>36</sup>

In another study a hot-pen was used to locally evaporate a hydrogen bonded chiral dopant from an LCN coating. After the coating was locally heated to 160 °C for 30 min, the reflection band in the heated areas was irreversibly shifted from 615 nm to 525 nm, revealing a readable written pattern. To increase resolution and reduce the time needed for the evaporation process, the coating was irradiated with a laser beam (700 mW cm<sup>-2</sup>) for

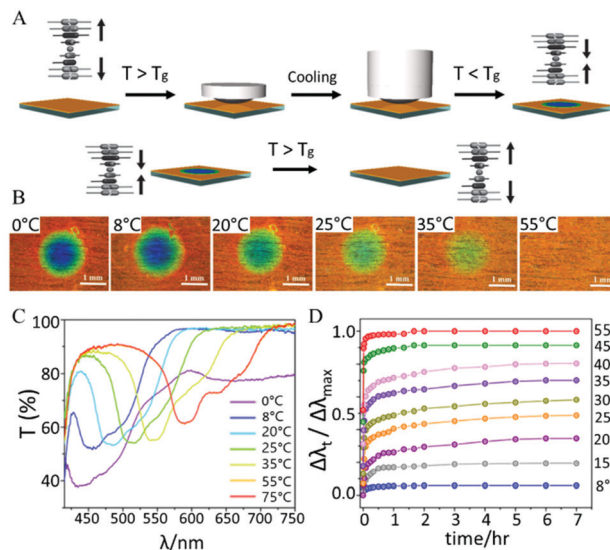


Fig. 2 (A) Schematic representation of embossing a shape memory cholesteric LCN polymer above  $T_g$  while cooling below  $T_g$  to compress the cholesteric pitch and induce a blue shift. Upon heating above  $T_g$  the pitch restores due to a shape memory of the network. (B) Images of the embossed area after maintaining the indicated temperature for 7 h. Scale bars are 1 mm. (C) The corresponding transmission spectra after maintaining the indicated temperature for 7 h. (D) Red shifts ( $\Delta\lambda_i$ ) of the embossed area measured at different temperatures over time normalized to the red shift observed at 75 °C ( $\Delta\lambda_{max}$ ). Adapted from ref. 35 (Copyright 2013 Wiley-VCH) and ref. 36 (Copyright 2017 ACS publications).

25 s, for which the local heating was enough to evaporate the chiral dopant showing a green to orange contrast with excellent resolution.<sup>37</sup> These coatings could be interesting as writable photonic paper.

### Two-way temperature responsive photonic polymers

**Temperature responsive hydrogels.** Although the intrinsically irreversible temperature responsive behaviour is sought after for *e.g.* time-temperature indicators and writable photonic paper, most envisioned applications, such as real-time sensors and thermochromic paints or windows, require a reversible color change. Gels (resp. hydrogels) can be used as responsive materials that can reversibly swell and de-swell in solvents (resp. water specifically) as function of temperature.

A well-known temperature responsive hydrogel is poly(*N*-isopropylacrylamide) (PNIPAM, Fig. 3A) which becomes more hydrophobic upon increasing the surrounding temperature above the so-called lower critical solution temperature (LCST). Monodisperse highly charged spherical PNIPAM particles were prepared by dispersion polymerization and organized in 3D photonic structure surrounded by water. Below the LCST (*ca.* 32 °C), PNIPAM particles were hydrated and swollen, and able to diffract light, whereas the PNIPAM hydrogel particles contracted and expelled water above the LCST, increasing thereby the films refractive index mismatch and reflection band intensity (Fig. 3B).<sup>38</sup> When PNIPAM particles are trapped inside the porous polystyrene matrix and can freely change their volume inside the pores, their organisation is disturbed when they shrunk





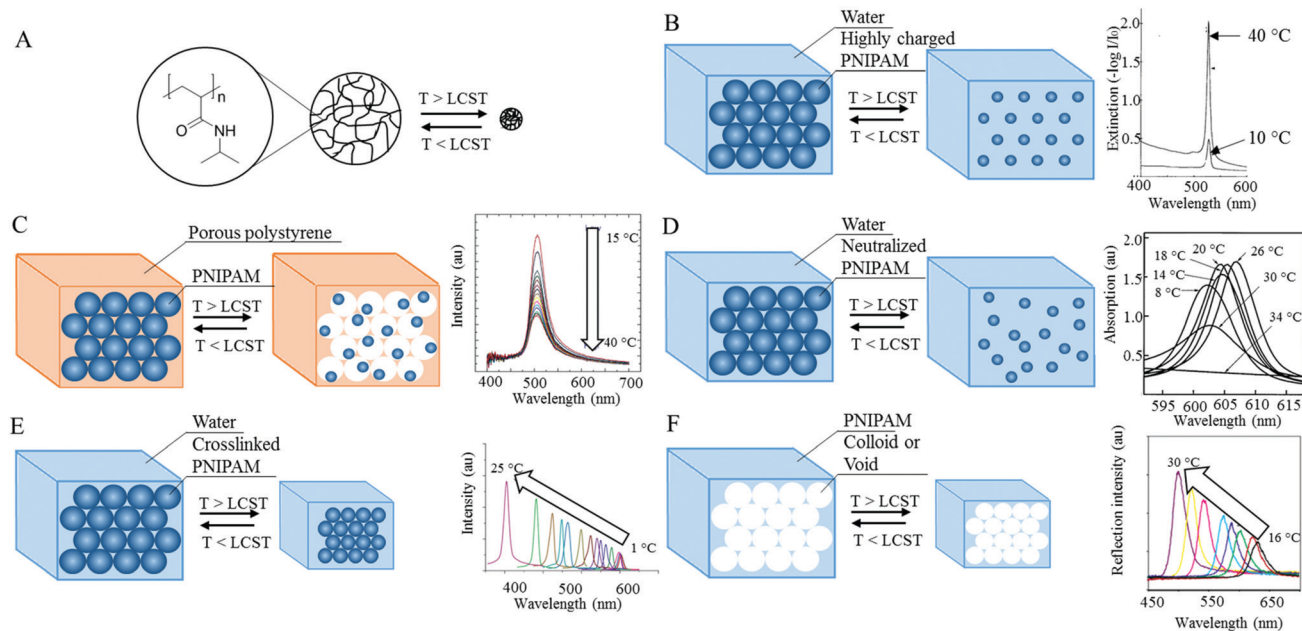


**Fig. 3** (A) Structure of PNIPAM. Below LCST the PNIPAM particle is hydrated and swollen, whereas above LCST the particle expels water and shrinks. (B) Closed-packed highly charged PNIPAM particles maintain their periodic structure above LCST resulting in a reflection band increase. Adapted with permission from ref. 38. Copyright 1996 AAAS. (C) Freely shrinking PNIPAM particles embedded in a porous polymer lose their periodic structure above LCST resulting in a decrease in reflection band intensity. Adapted with permission from ref. 39. Copyright 2006 ACS publications. (D) For neutralized closed-packed PNIPAM particles the periodic structure collapses above LCST resulting in transition to an opaque state. Adapted with permission from ref. 40. Copyright 2000 ACS publications. (E) Crosslinked closed-packed PNIPAM particles maintain their periodic structure when shrinking above LCST resulting in a blue shift. Adapted with permission from ref. 42. Copyright 2013 Wiley-VCH. (F) Inverse opal PNIPAM structures also maintain their periodic structure above LCST resulting in a blue shift. Adapted with permission from ref. 43. Copyright 2001 Wiley-VCH.

and an approximately 3-fold decrease in reflection band intensity was observed upon increasing the temperature from 15 to 40 °C (Fig. 3C).<sup>39</sup>

In closed-packed neutralized PNIPAM particles, an order-disorder transition led to a reversible non-opaque to opaque transition upon crossing the LCST (26 to 34 °C). Since these particles lack Coulombic repulsion forces, they cannot maintain their periodic photonic structure upon shrinkage and collapse resulting in an opaque state (Fig. 3D).<sup>40</sup> By connecting closed-packed PNIPAM particles with a covalent crosslinker they could be stabilized.<sup>39,41,42</sup> Upon heating, these particles could maintain their structural order before collapsing, which leads to a blue shift upon heating to 31 °C followed by an opaque state upon subsequent heating to 50 °C. In addition, since the network restores its original conformation elastically, the initial colour was restored within 10 s, which was 1000 times faster compared to a non-crosslinked assembly.<sup>41</sup> Crosslinked closed-packed PNIPAM particles blue shifted from 700 to 400 nm upon heating from 1 to 25 °C was accompanied by an approximately 6-fold intensity increase, due to an enhanced refractive index mismatch (Fig. 3E).<sup>42</sup> A similar response was observed for inverse opal PNIPAM hydrogels. For fabricating this polymer, a pre-hydrogel monomer solution was added to a 3D photonic structure made from 210 nm silica spheres. After polymerization of the monomer solution the template was removed, *via* etching, and an inverse opal photonic structure with periodically arranged voids surrounded by a hydrogel polymer matrix

was left. This photonic PNIPAM hydrogel showed a blue shift up to 200 nm accompanied by an intensity increase (Fig. 3F).<sup>38,43</sup> The photonic structures could also be fabricated using top-down lithography. HEMA-based inverse opal structures were fabricated using interference lithography, which showed a blue shift of 120 nm, accompanied by a reflection band intensity cut when going from 25 to 50 °C due to a decreased air cavity volume fraction.<sup>44</sup>

A hydrogel that blue shifts over the entire visible range, from 800 to 450 nm, upon heating from 23 to 49 °C was obtained by fabrication of 1D photonic structure (structure schematically depicted in Fig. 1). These Bragg gratings were prepared *via* layer-by-layer stacking of a non-responsive polymer and a responsive hydrogel (*e.g.* PNIPAM). To have a good balance between processing time and reflectivity a stack of 11 layers was prepared.<sup>45</sup> To reduce the number of layers required to get a sufficient reflection band, the refractive index contrast between the layers was enhanced by intercalating inorganic layers or doping polymer layers with inorganic particles, such as TiO<sub>2</sub> or ZrO<sub>2</sub>.<sup>46,47</sup> Besides a less labour intensive process, doping with inorganic particles also provides a way for the fabrication of all-gel Bragg reflectors consisting of PNIPAM and PNIPAM doped with inorganic particles. All-gel Bragg reflectors might be desirable for the mechanical properties as well as the speed of mass transport of large polar molecules for chemical or biological sensing applications compared to the use of brittle and hydrophobic non-hydrogel polymers, such as poly(*para*-methyl-styrene).<sup>47</sup>



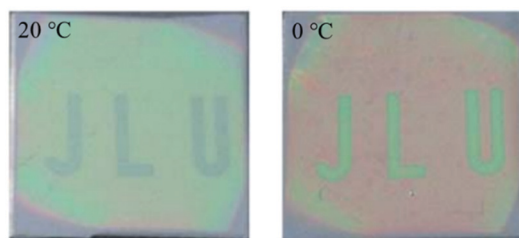


**Fig. 4** Bragg grating based on PNIPAM, which is prewritten by illuminating the letters (J, L and U) for 2 minutes with UV light, while the surrounding area is not illuminated. The pattern changes colour when using water of different temperatures as is shown here for 20 and 0 °C. Adapted from ref. 48 with permission from The Royal Society of Chemistry.

By increasing the crosslinking time of hydrogel-based Bragg stacks from 0 to 3 minutes, the swelling behaviour of the gel was reduced, resulting in a blue shifted reflection band from 609 to 532 nm. Using this effect photonic paper could be made of which the pattern could be prewritten using photolithography. The pattern appeared when submerging the hydrogel in water and erases upon drying. The colour of the letters could be changed by using water of different temperature between 0 and 20 °C as ink (Fig. 4).<sup>48</sup>

Other temperature responsive photonic hydrogels rely on reversible hydrogen bonding as driving force for thermochemical properties. Gong *et al.* self-assembled a lamellar structure with a periodicity of several hundreds of nanometres of hard poly(dodecylglyceryl itaconate) (PDGI) bilayers and a soft poly(acrylamide) (PAAm) network matrix. The parent gel was immersed in an aqueous solution of acrylic acid (0.5 M), which associates with the PAAm layer *via* hydrogen bonding. After polymerization of the acrylic acid, an interpenetrating PAAm–PAAc network was formed. With increasing temperature from 5 to 40 °C the hydrogen bonds dissociate, causing swelling of the soft layer and hence a redshift of the reflection band from 400 to 700 nm.<sup>49</sup>

**Temperature responsive block copolymers.** Block copolymers can also be used to make temperature responsive photonic materials. Polystyrene-*block*-poly(4-vinylpyridinium methane-sulphonate) block copolymers were complexed with a hydrogen bonding solvent (3-*n*-pentadecylphenol), specific for one of the polymer blocks. Upon heating from 80 to 134 °C, hydrogen bonds were broken and the solvent became non-specific, which induced a decrease in periodicity of the lamellar structure and thus a blue shift from 530 to 370 nm.<sup>50</sup> These responsive photonic systems cover the entire visible range and are therefore seen as promising for sensors in water environments or rewritable paper using water as ink.

**Temperature responsive liquid crystal polymers.** Cholesteric LC polymers are another class of polymers suitable for reversible temperature responsive behaviour. As discussed before, LCNs are used as irreversible shape memory polymers. By incorporating LC elastomers (LCEs), reversible temperature responses were also realized. LCEs, such as side chain liquid crystalline polysiloxanes (SCLCPs), were combined with chiral LC monomers, to form a semi-interpenetrating (semi-IPN) network after UV-polymerization. These coatings showed a reversible

decrease in reflection band intensity upon heating above the cholesteric-to-isotropic transition temperature of the elastomer, due to loss of the cholesteric organization of the elastomer. The wavelength reflected was tuned between 500 and 900 nm by varying the concentration of chiral LC monomers. The reflectivity loss upon heating could be tuned by varying the crosslink density. Upon heating from 20 to 120 °C, 49 to 94% of the reflectivity was lost when decreasing the concentration of monomers in the mixture from 25.5 to 14.9 wt%, respectively. The reflectivity was recovered upon cooling. (Fig. 5).<sup>51</sup>

Other temperature responsive photonic elastomers showed a blue shift with increasing temperature, owing to an LC phase transition. For instance, SCLCPs were prepared with a cholesteric to blue phase transition at 126 °C. Blue phases are distinct thermodynamic LC phases that appear over a narrow temperature range at the cholesteric to isotropic boundary of highly chiral LCs.<sup>52</sup> Getting closer to the blue phase the cholesteric pitch became shorter and thus blue shifted. Wavelength shifts between 525 and 406 nm were obtained this way.<sup>53</sup> Larger shifts

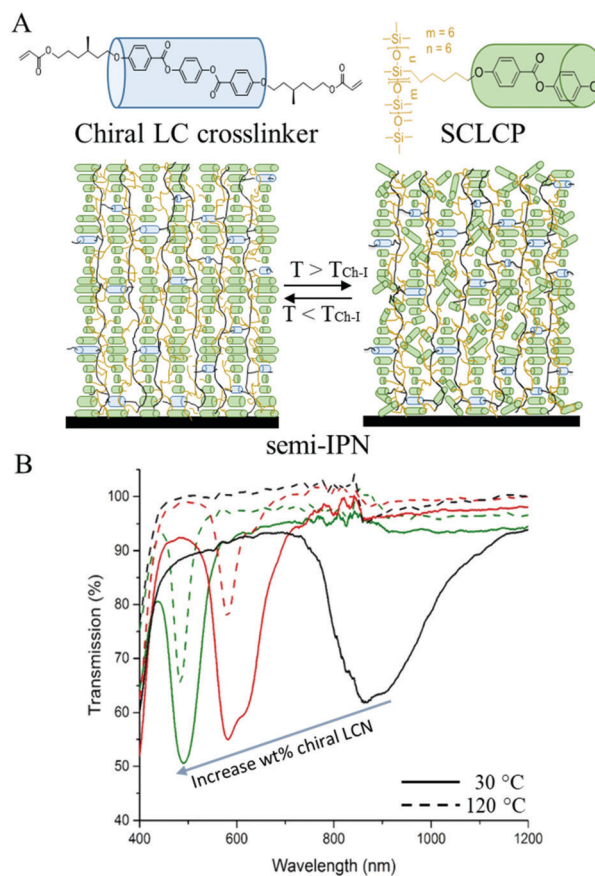


**Fig. 5** (A) Schematic representation of a semi-IPN formed by an SCLCP interpenetrating through a cholesteric LCN. Upon heating above the  $T_{Ch-I}$  the SCLCP loses cholesteric order, which it gains again upon cooling below  $T_{Ch-I}$  (B) transmission spectra showing the reversible decrease of the reflection band intensity of coatings containing various concentrations of chiral LCN. The solid lines represent the spectra at 30 °C and the dashed lines the spectra at 120 °C. Chiral dopant concentration were 14.9, 21.0, 25.5 wt% for the black, red and green curves, respectively. Adapted with permission from ref. 51. Copyright 2018 Wiley-VCH.



are found for LC elastomer materials with a smectic to cholesteric transition. A smectic LC phase does not have a helical structure, such as a blue phase, and can therefore be considered as an infinite long pitch. Therefore getting close to the cholesteric to smectic transition upon cooling results in an enormous red shift. That is why a mixture of an SCLCP with a low molecular weight chiral dopant having this transition resulted in a polymer film that shifted reversibly from 1250 to 2350 nm upon cooling from 57 to 17 °C.<sup>54</sup> Another material having a smectic to cholesteric transition was obtained by coating short oligomers of reactive LCs. This yielded coatings that could shift between 1195 and 701 nm or between 754 to 484 nm, covering thereby the entire visible range. These large blue shifts upon heating do not only make these materials potentially attractive for decorative and sensing applications, but also as energy saving infrared regulating smart windows.<sup>55</sup> Furthermore these materials can be coated using conventional coating techniques, such as blade-coating, which increase their potential for large scale coating products.

A drawback of these materials is that they are relatively soft and therefore prone to damage. To fabricate a more mechanically robust system cholesteric LC droplets can be embedded inside a hard polymer network. The composition of these LC droplets can be chosen in such a way that they show a colour change from red to blue upon heating within the cholesteric phase, after which they become isotropic upon further heating. By varying the LC ink composition the transition temperatures can be controlled. This concept, first patented in 1975 by Robert Parker Research, has been used to fabricate all kinds of thermometers, such as forehead strips, colour changing labels and mood rings.<sup>56</sup> Such polymer dispersed liquid crystals show great potential for scalability using flexible substrates and a roll-to-roll process. Liang *et al.*, showed the successful fabrication of meter scale temperature responsive foils.<sup>57,58</sup> However, although these systems are based on a liquid crystalline phase transitions, no aligned cholesteric phase was obtained and therefore, these particular systems are based on scattering mechanisms instead of photonic reflection.

## Humidity responsive photonic polymers

Optical humidity sensors can be fabricated by incorporating hydrophilic polymers containing polar or charged moieties in various photonic structures. This creates two-way responsive photonic polymer films that can swell and de-swell depending on the humidity of the environment.

### Two-way humidity responsive photonic polymers

**Humidity responsive hydrogels.** Humidity responsive colloidal coatings have been prepared by incorporating colloidal particles into a responsive hydrogel polymer matrix.<sup>27,59–61</sup> Due to the swelling of the matrix upon water/vapour absorption the spacing between the colloidal structures increased, causing a red shift of the reflected wavelength. A fully polymeric coating was reported in which monodisperse poly(styrene-*co*-methyl

methacrylate-*co*-acrylic acid) latex particles were crystallized on a glass substrate and embedded in a poly(acrylamide bis(acrylamide)) matrix. By increasing the humidity from 20 to 100%, the coating was able to swell reversibly from 6 to 15 μm thickness. This results in a shift of the reflection band from 390 to 630 nm, respectively, covering nearly the entire range of visible light. Only minor fluctuations between at least 10 cycles were observed upon increasing and lowering the relative humidity, showing good reversibility.<sup>59</sup>

Others used inorganic colloids, such as monodispersed silica nanoparticles (Si-NPs). Yang *et al.*, showed the ability to create a photonic humidity sensor by spray-coating a mixture of polyvinyl alcohol (PVA) solution and Si-NP latex with ultrapure water and ethanol. The dispersed Si-NPs self-assembled into a photonic structure with PVA and Si-NP as the solvent evaporates. Fast (<1 s) 60 nm shifts of the reflection band due to swelling of the PVA were observed when exposing the coating reversibly to vapour and nitrogen (Fig. 6).<sup>60</sup>

Larger shifts of the reflection band were achieved by a nanoporous polymer films of poly(ethylene glycol diacrylate).<sup>62</sup> 275 nm colloidal Si-NPs were assembled on a substrate, immersed in the photo curable polymer and removed by etching after polymerization. After plasma-treatment of the inverse opal film to increase the hydrophilicity, the resulting humidity sensor showed a red shift of 137 nm upon increasing the humidity from 25 to 98% RH by water uptake of the cavities in the film, making them more suitable for discrimination by human eyes. Comparable responses were also obtained by deposition of alternating poly(2-hydroxyethyl methacrylate) and TiO<sub>2</sub> layers on various substrates.<sup>17</sup> Due to the absence of heat, radiation, or damage induced by solvents during preparation, there is

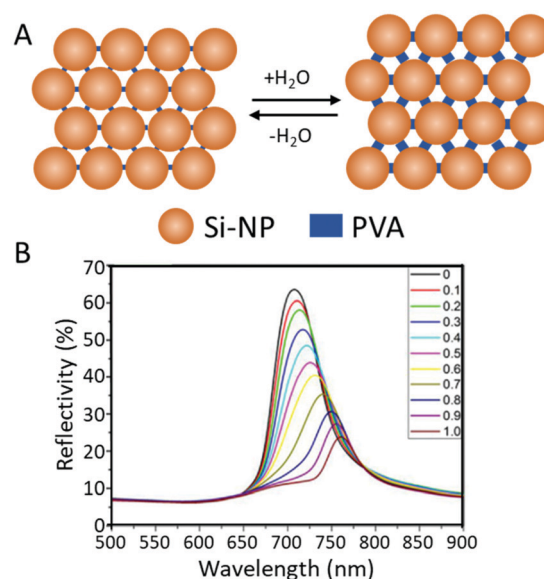


Fig. 6 (A) Schematic illustration of the periodic structure change of PC hydrogel before and after being wetted by water. (B) UV-vis spectra of the films under various concentrations of water vapor. Each of these curves correspond to varying concentrations of water in the medium from 0 and 100%. Adapted with permission from ref. 60, copyright 2017 Elsevier.





freedom in terms of substrate choice. Moreover, only 0.3 s are needed for the coatings to undergo a colour change from green to red, caused by 1 mol% water vapour in  $N_2$ . The rapid and reversibly tunable reflectance and scalable production techniques make also these materials good contenders for real-time humidity sensing applications.

A different approach was used when a humidity sensor was fabricated using holographic patterning of polymer-dispersed liquid crystals.<sup>63</sup> Alternating layers of nanoporous and non-porous regions were created. After water uptake in the nanoporous layers, the refractive index mismatch between the layers decreased, the position of the reflection band slightly red shifted and the transmittance at the reflective wavelength increased. Increasing the humidity from 40% to 95% RH at a constant temperature of 34 °C, the relative transmittance was increased from 12% (almost opaque) to 87% (transparent) in only a few seconds, which is highly stable for multiple cycles with only minor hysteresis. These sensitive, robust, quickly responding and cost efficient coatings are interesting for RH sensing applications. However, due to the lack of a reflection band shift and thus visible colour change they require a monitoring system to discriminate between various RH levels.

**Humidity responsive block copolymers.** Another type of humidity responsive coatings that are able to cover nearly the entire visible light spectrum from violet to red at 20 to 95% RH, respectively, is made of periodically structured self-assembled block copolymers (Fig. 7).<sup>64</sup> Hexagonally packed hydrophobic polymethylbutylene cylinders were embedded in a hydrophilic polystyrene-sulfonate (PSS) matrix, resulting in photonic films with a thickness of 240 nm. Because of this hexagonal cylindrical morphology, a short diffusion pathway of water molecules in the PSS matrix is created, causing fast response times of only a few seconds. The magnitude of the shift strongly depends on the sulfonation level in the PSS, in which higher a sulfonation levels causes a larger red-shift of the reflection band. By combining the fast response times with the visually readable colour changes, these materials may be interesting for real-time humidity sensors monitoring with high susceptibility.

**Humidity responsive liquid crystal polymers.** Humidity responsive coatings based on hydrogen-bond-containing cholesteric

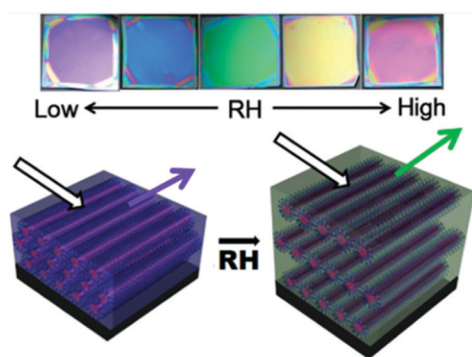


Fig. 7 Photographs of a coating at various RH showing the colour changes and a schematic representation of the working principle. Adapted with permission from ref. 64. Copyright 2012 ACS publications.

LCNs are able to absorb water from their environment after the hydrogen bonds are treated with potassium hydroxide (KOH) solution to create hygroscopic polymer salts.<sup>65</sup> The helical pitch of the cholesteric LCN increases because of the water absorption, shifting the reflected light to longer wavelengths. A visible colour shift from green to yellow was observed when the RH was increased from 3 to 83%. Patterns were realized by illumination through masks or inkjet printing of  $Ca^{2+}$  containing solutions. Upon water uptake, inhomogeneous swelling occurred, creating various colours in one sample. The creation of photonic images, make these materials potentially suitable for customizable aesthetics, data encryptions and anti-counterfeit labels.<sup>21,66</sup> Fully camouflaged films were prepared using inkjet printing of  $Ca^{2+}$  ion aqueous solutions on a coating after removal of nonreactive monomers and a base treatment using a 1 M KOH solution. By replacing monovalent potassium ions by a bivalent calcium ion, swelling is inhibited, since it re-established the connection between two carboxylate anions (Fig. 8A). Patterns appear after breathing or water dipping. As illustrated in Fig. 8B, higher concentrations of  $Ca^{2+}$  ensured a lower degree of swelling of the

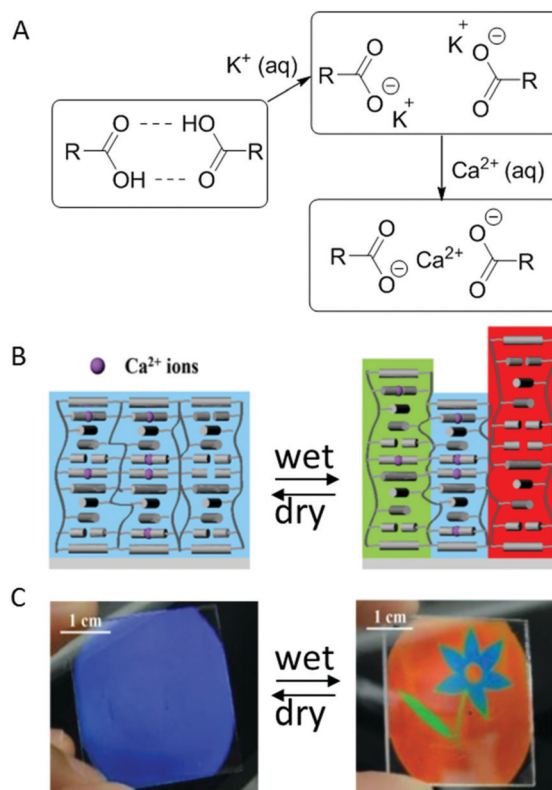


Fig. 8 (A) Hydrogen bonds are disrupted by treatment with  $K^+$  ions, upon saturating the coating with  $Ca^{2+}$  swelling with water is inhibited due to the re-establishment of the connection between the carboxylate anions. (B) The coating is patterned by saturating different spots to different levels. In the wet state, areas with lower amounts of  $Ca^{2+}$  ions swelled more compared to more saturated areas, giving rise to full colour patterning while staying indistinguishable from each other in a dry blue-coloured state. (C) Image of an inkjet-printed full colour flower pattern which appeared in the wet state, but was hidden in the dry state. Adapted with permission from ref. 21. Copyright 2018 ACS publications.



coatings when exposed to water or vapour, enabling formation of camouflaged multi-coloured images (Fig. 8C).

A similar effect was achieved using a co-assembly of acid-hydrolyzed photonic cellulose nanocrystals (CNCs) and waterborne polyurethane (WPU).<sup>67</sup> After writing on the films with a 0.025 M NaCl solution, patterns were visualized by exhaling. Choosing different inks such as water or 0.1 M NaCl, the patterns could also be made temporary (irreversibly removed upon drying) or more durable (still visible when dried), respectively. By washing the film with water, patterns were erased and could be written again, making these materials promising as rewritable paper. Similar research on free standing films showed that by including 10 to 30 wt% polyethylene glycol larger reversible shifts of approximately 435 nm could be achieved when increasing the RH from 30 to 100%. Simultaneously the intensity of the reflection band is decreased.<sup>68</sup> This results in the ability to obtain a broader spectrum of colours, ranging from green to red and even to colourless materials at high RH.

## Light responsive photonic polymers

Infiltrating photonic polymers with photochromic dyes enables the ability to create reversible, two-way light responsive materials. Well-known photo responsive moieties are azobenzenes and spiropyrans. These moieties can undergo an isomerization upon light irradiation causing change in size and conformation of the photochromic dye. By using azobenzenes, a *cis-trans* isomerization is observed,<sup>69</sup> whereas spiropyrans give rise to the open-ring isomer merocyanine upon UV-illumination (Scheme 1).<sup>70</sup>

### Two-way light responsive photonic polymers

**Light responsive gels.** Photo-responsive hydrogels were prepared by incorporating a photochromic dye into hydrogel copolymers.<sup>71–73</sup> Azobenzene moieties were covalently linked through a maleimide–thiol linker to polymerized polystyrene colloids of 120 nm, arranged in a photonic colloidal array (CCA). Upon UV light illumination ( $13 \text{ mW cm}^{-2}$ ), the free energy of mixing of the hydrogel polymer network with the medium (dimethylsulfoxide (DMSO)) increases as a result of difference in miscibility between the *cis*- and *trans*-isomers (Fig. 9). The expansion of the CCA causes a red shift of the reflection band, while a blue shift results from a decrease of free mixing upon return of the *trans*-isomerized azobenzene. The magnitude of the diffraction shift increases with increasing

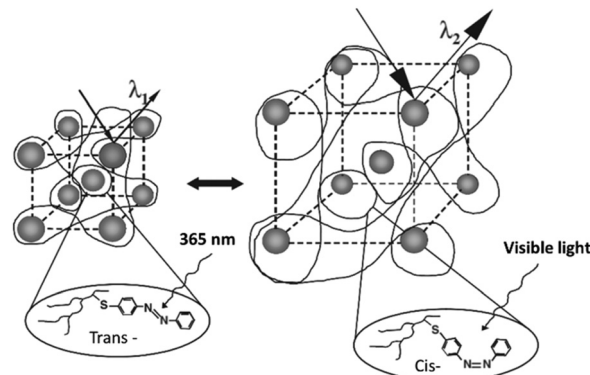


Fig. 9 Schematic representation of the CCA and its photo-responsive behaviour. UV light photo-isomerizes the *trans* to the *cis* derivative, while visible light photo-isomerized the *cis* to the *trans* form. Due to better miscibility of the *cis* isomer in DMSO, swelling occurs causing a red shift of the photonic reflection band. Adapted with permission from ref. 71. Copyright 2003 Wiley-VCH.

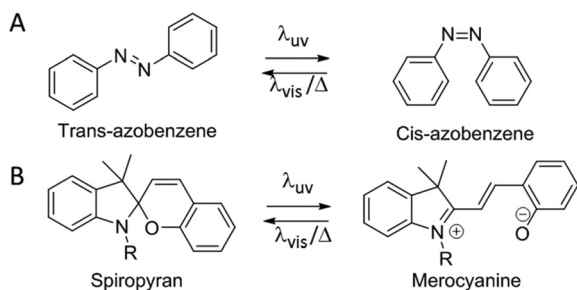
azobenzene concentration and decreases as the hydrogel cross-linking density increases. Using 4.5 mM azobenzene and low crosslink concentration ( $< 2\%$ ), a 60 nm red shift was observed between 500 and 600 nm, with a reversible shifting response in the order of seconds to minutes.<sup>71</sup>

Using spiropyran in polymerized 135 nm polystyrene colloids arranged in a CCA and dissolved in DMSO, an approximately 10 nm (669 nm to 679 nm) shifting behaviour with switching times in the order of seconds to minutes is caused by the change in charge localization of the spiropyran and merocyanine.<sup>72</sup> A higher charge localization is created while isomerizing to the open-ring form, causing again a reversible increase in free energy of mixing of the hydrogel polymer network in the solvent and thus red shift of the reflection band.

**Light responsive liquid crystal polymers.** Photo-responsive LC films were prepared by a  $\text{SiO}_2$  inverse opal, filled with non-reactive nematic LC, including an azobenzene-based LC.<sup>74,75</sup> Upon illumination with UV-light, the azobenzene moieties isomerize from *trans* to *cis*, causing a nematic-to-isotropic transition of the LC inside the voids of the inverse opal film. In the nematic phase, the LCs were aligned parallel to the voids surface forming random bipolar orientations with respect to each other. Since the dielectric constants of the LC spheres were random, requirements for Bragg diffraction were not met, leading to light scattering.

In the isotropic phase, the dielectric constant became equal for all voids and a reflection peak due to Bragg diffraction appeared (Fig. 10A). After several seconds a clear reflection band became visible, which disappeared after the illumination was stopped or illuminated wavelength was changed to visible light (Fig. 10B). Since thermotropic liquid crystals were used, a phase-transition to the isotropic phase could also be obtained by temperature (from  $25 \text{ }^\circ\text{C}$  to  $40 \text{ }^\circ\text{C}$ ), making these systems dual-responsive.<sup>75</sup>

Zhao *et al.*, used a similar approach in which the inverse opal film itself was prepared from polymerizable LCs including an azobenzene-based LC.<sup>76</sup> Upon light exposure, the alignment



Scheme 1 (A) *cis-trans* isomerization of azobenzene. (B) Ring opening isomerization of spiropyran to merocyanine.





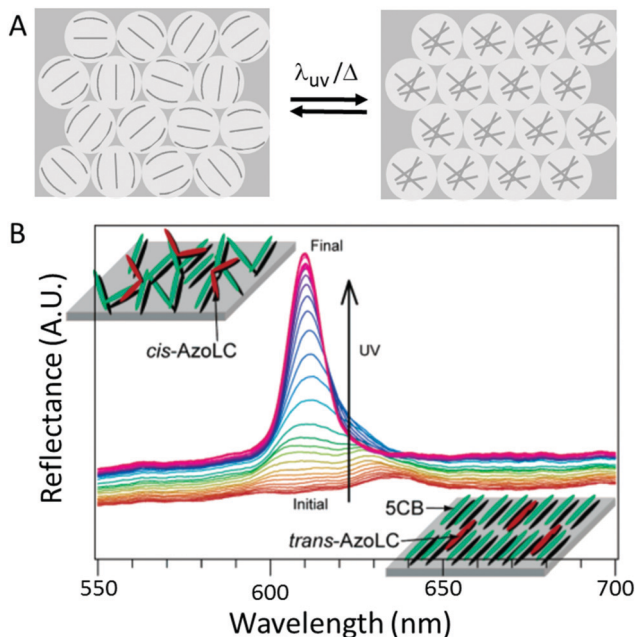


Fig. 10 (A) Schematic representation of the random bipolar (left) and isotropic (right) alignment. (B) Reflection spectra of a mixture of 5CB and AzoLC-infiltrated inverse opal films. Upon illumination with UV-light, a peak appears due to the disruption of the nematic alignment, which is caused by the *cis*-isomers. Adapted with permission from ref. 75. Copyright 2004 ACS publications.

of the polymers is disrupted and the order of the inverse opal film is reduced. Therefore, these films behave in an opposite way to the SiO<sub>2</sub> filled with LCs, meaning that upon UV-illumination (5 min, 365 nm, 50 mW cm<sup>-2</sup>) the reflection band nearly disappears and recovers during visible light illumination (15 min, 530 nm, 20 mW cm<sup>-2</sup>). An intensity contrast of more than 77% was reached. Again, a dual-responsive system was created, since the reversible phase-transition could also be induced by temperature.

Another approach to inhibit Bragg reflection in an ordered system is to match refractive indices. To achieve this, glass substrates were spincoated with alternating layers of azobenzene polymer liquid crystals and poly(vinyl alcohol).<sup>77–79</sup> Photonic reflectance was lost after annealing at 80 °C, because of the thermal-induced out-of-plane molecular orientation of the azobenzene polymer, causing a very small difference in refractive indices between the different layers.<sup>77</sup> The out-of-plane orientation of the azobenzene polymer was also obtained using visible light of 436 nm (60 mW cm<sup>-2</sup>) for 1 hour (Fig. 11A and B).<sup>78</sup> In both cases, the azobenzene polymers could reorient to an in-plane random orientation, leading to an increase in reflectivity from approximately 20 to 80% using 365 nm UV-light between 8 and 40 mW cm<sup>-2</sup> for 5 minutes. The reflectivity increase can be improved by approximately 10% after illumination of 5 minutes by copolymerizing high refractive non-photo-responsive LC groups, which prevents interruption of light penetration needed for the photo-response.<sup>78,79</sup> Patterned coatings were prepared by illumination through a mask, which were stable for more than a few weeks at room

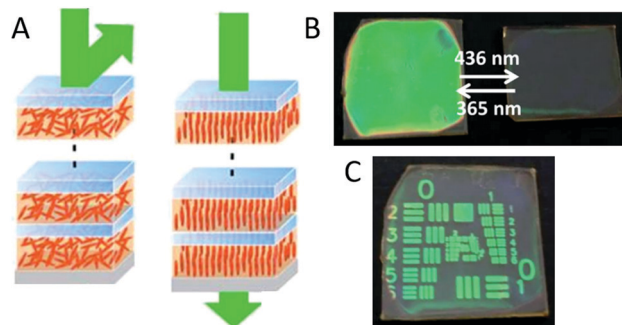


Fig. 11 (A) Schematic representation of the changes in molecular orientation of the azobenzene polymers, showing the in-plane random orientation after exposure to 365 nm light (left) and the out-of-plane orientation after exposure to 436 nm light (right). (B) Photographs of the coating for both the in-plane random and out-of-plane orientation of the azobenzene polymers. (C) Photograph of a patterned coating, prepared by illumination through a mask. Adapted from ref. 78 with permission from The Royal Society of Chemistry.

temperature and ambient light (Fig. 11C). Moreover, reflected colour and intensity could be tuned by layer thicknesses, in which thicker layers enabled reflectance at higher wavelengths, and bilayer numbers, in which an increase in layers ensured an increase in intensity of the reflection band. The reversibility, stability and pattern-ability make these materials potential candidates for photo-rewritable paper and cell-free, self-standing reflective colour display devices without backlight.

In order to shift the reflected wavelength instead of increasing or decreasing its intensity, an inverse opal structure was created based on azobenzene containing polymers.<sup>80</sup> Upon irradiation with linearly polarized light, the out-of-plane orientation of the azobenzene moieties parallel to the incident light increase. Therefore, the effective refractive index of the azobenzene polymers was decreased by 0.034 according to calculations. As a result, the photonic bandgap was blue-shifted with increasing irradiation time, obtaining a maximum shift of 40 nm after 25 minutes illumination with 488 nm light at a fixed intensity of 100 mW cm<sup>-2</sup>.

## Conclusions and future challenges

Academic research has shown beautiful examples of adaptive photonic polymer coatings that autonomously respond to environmental stimuli as temperature, humidity and light, similar to environmentally adaptive photonic structures found in nature. Across these polymers, various mechanisms are responsible for the structural colour change, including polymers that show a shape memory, hydrogels and block-copolymers that can swell and de-swell and liquid crystal polymers that can undergo a phase transition or change in order. Table 1 categorizes the responsive polymers highlighted in this feature based on their response mechanism. This table also lists the responsive properties and their potential applications. In this section we will discuss the feasibility and challenges of these materials in future applications.



**Table 1** An overview of various environmental stimulus-responsive photonic polymer materials categorized by their responsive mechanism. Their maximum responses as well as additional information on their processing techniques, potential applications and limitations is provided

	One-way stimuli-responsive polymer	Two-way stimuli-responsive polymers using a solvent	Reversible stimuli-responsive polymers without the need of a solvent
Working mechanism	Recovery of original shape	Swelling of the polymer by a solvent	Phase transition or change in order
Stimulus	Temperature	Temperature, humidity and light	Temperature and light
Maximum responses	Temperature: red shift (200 nm upon heating from 10 to 1 °C, ref. 36)	Temperature: reflectivity change (3-fold increase or decrease upon heating from 10 to 40 °C, ref. 38 and 39) Blue shift (350 nm upon heating from 23 to 49 °C, ref. 45)  Humidity: red shift (240 nm upon increasing from 20 to 100% RH, ref. 59) Reflectivity decrease (about 75 to 12% upon increasing from 40 to 95% RH, ref. 63)  Light: red shift (60 nm upon radiation with UV-light of 13 mW cm <sup>-2</sup> for 2 minutes, ref. 71)	Temperature: reflective to transparent (94% reflectivity loss upon heating from 20 to 120 °C, ref. 51) Transparent to opaque (about 70% transmission decrease upon heating from 27 to 35 °C, ref. 58) Blue shift (1100 nm upon heating from 17 to 57 °C, ref. 54) Light: reflectivity decrease (about 90 to 20% upon radiation with UV-light of 50 mW cm <sup>-2</sup> for 5 minutes, ref. 76)
Speed of responses	Minutes to years	Seconds to minutes	Seconds to hours
Potential applications <sup>a</sup>	Time-temperature integrator, temperature sensor, rewritable paper	Optical sensors, rewritable paper, chemical sensors, aesthetics, data encryption, anti-counterfeit labels	Optical sensors, aesthetics, energy saving smart windows, photo-rewritable paper, reflective colour displays

<sup>a</sup> Mentioned in reference cited in the present article.

One-way responsive shape memory photonic polymers can be processed in monomeric state *via* blade-coating or printing after which they need to be embossed to trigger a shape memory effect. These processing techniques are suitable for large-scale production. Further development of these materials regarding industrialization would be to process them *via* roll-to-roll compatible processes on various substrates. Photonic hydrogels are mostly fabricated *via* lab-scale techniques. A few examples already exist that use scalable techniques such as spray- and blade-coating of self-assembled colloidal (hydrogel) particles.<sup>60,81</sup> Another option to produce photonic hydrogels is to fabricate the hydrogel structures *via* layer-by-layer stacking, which is usually done by spin-coating subsequent layers. At lab-scale, this technique has the advantage of controllable layer thicknesses and free choice of materials. However, for larger-scale production, thickness control is challenging. To be able to process LC elastomers with coating techniques such as blade-coating, the addition of (polymerizable) low molecular weight liquid crystals is required, an addition that also provides the ability to control the responsive properties of these materials by varying the coating formulation.

Among the polymers that can swell and de-swell, photonic hydrogels are the most commonly used to create adaptive photonic polymers. By using temperature or humidity as a stimulus, large responses with respect to reflectivity as well as central wavelength position can be achieved. These features are of interest for potential applications in technologies such as sensors, aesthetics and rewritable paper. However, these materials are limited to

(biomedical) applications that involve wet environments, since they require water. Responsive photonic polymers can also be fabricated that operate without a swelling solvent. Elastomeric materials will be prone to damage, leaving for instance fingerprints upon touching. For commercial applications, this may require the need of, for instance, a protective coating or the need to coat the LCE on the interior of a double pane window. A more commercially established technique is the use of LC droplets embedded in a polymer binder, which provides mechanical robustness. This technology is already used for temperature sensors for decades and recently also steps in the direction of smart windows have been taken.<sup>56,58</sup>

For many applications the responsive properties of photonic materials needs to be fine-tuned. For example, for smart window applications in buildings, greenhouses and car interiors, temperature-responsive IR reflecting polymers could be of interest in order to minimize indoor heating, with fast response times in the order of minutes or even seconds. In most light responsive photonic polymers, high energy UV-light is required and thereby the lifetime of the materials is potentially limited, due to degradation. Thus obtaining polymers responsive to lower energy light (*e.g.* ambient sunlight) is a highly desirable goal in this field of research. Other applications, such as biomedical, would benefit from materials that are responsive towards visible light instead of UV-light.

To conclude, environmental stimulus-responsive photonic polymer films can be fabricated that respond to temperature, humidity or light. Similar to self-regulating processes in



organism, these coatings have the potential to be used in for example communication (displays), indoor temperature maintenance (energy saving smart windows) and camouflage (security labels). To exploit this potential and to bridge the gap between academic research and industry, stability, fatigue and processing techniques should get extra attention as well as adhesion of the coatings with various substrates. Research in this field is already initiated by several scientists and is likely to grow in the coming years.<sup>82,83</sup> This would provide a way to implement environmentally responsive photonic polymers in various coating applications.

## Conflicts of interest

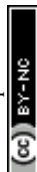
There are no conflicts to declare.

## Acknowledgements

The authors would like to acknowledge the inspiring discussions with and contributions of all current and former colleagues. This research was financially supported by Saudi Basic Industries Corporation (SABIC) and the Netherlands Organization of Scientific Research (NWO). This work was further financially supported by the National Natural Science Foundation of China (No. 51561135014, U1501244, 2161101058), the Program for Changjiang Scholars and Innovative Research Teams in Universities (No. IRT13064) and the Guangdong Innovative Research Team Program (No. 2013C102), the Major Science and Technology Projects of Guangdong Province (No. 2015B090913004), the 111 Project, the Collaborative Innovation and Platform for the Construction of special funds of Guangdong Province (No. 2015B050501010), and the SCNU-TUE Joint Lab of Devices Integrated Responsive Materials.

## Notes and references

- 1 A. Grinthal and J. Aizenburg, *Chem. Soc. Rev.*, 2013, **42**, 7072–7085.
- 2 H. Chou, A. Nguyen, A. Chortos, J. W. F. To, C. Lu, J. Mei, T. Kurosawa, W. Bae, J. B. Tok and Z. Bao, *Nat. Commun.*, 2015, **6**, 1–10.
- 3 J. Sun, B. Bhushan and J. Tong, *RSC Adv.*, 2013, **3**, 14862.
- 4 S. Tadepalli, J. M. Slocik, M. K. Gupta, R. R. Naik and S. Singamaneni, *Chem. Rev.*, 2017, **117**, 12705–12763.
- 5 H. Wang and K. Q. Zhang, *Sensors*, 2013, **13**, 4192–4213.
- 6 T. Lu, W. Peng, S. Zhu and D. Zhang, *Nanotechnology*, 2016, **27**, 1–14.
- 7 H. Fudouzi, *Sci. Technol. Adv. Mater.*, 2011, **12**, 064704.
- 8 J. Ge and Y. Yin, *Angew. Chem., Int. Ed.*, 2011, **50**, 1492–1522.
- 9 A. Seeboth, R. Ruhmann and O. Mühlhng, *Materials*, 2010, **3**, 5143–5168.
- 10 A. Seeboth, D. Löttsch, R. Ruhmann and O. Muehling, *Chem. Rev.*, 2014, **114**, 3037–3068.
- 11 J. E. Stumpel, D. J. Broer and A. P. H. J. Schenning, *Chem. Commun.*, 2014, **50**, 15839–15848.
- 12 C. I. Aguirre, E. Reguera and A. Stein, *Adv. Funct. Mater.*, 2010, **20**, 2565–2578.
- 13 N. Akamatsu, K. Hisano, R. Tatsumi, M. Aizawa, C. J. Barrett and A. Shishido, *Soft Matter*, 2017, **13**, 7486–7491.
- 14 L. Nucara, F. Greco and V. Mattoli, *J. Mater. Chem. C*, 2015, **3**, 8449–8467.
- 15 I. B. Burgess, M. Lončar and J. Aizenberg, *J. Mater. Chem. C*, 2013, **1**, 6075.
- 16 M. Moirangthem, A. F. Scheers and A. P. H. J. Schenning, *Chem. Commun.*, 2018, **54**, 4425.
- 17 M. Karaman, S. E. Kooi and K. K. Gleason, *Chem. Mater.*, 2008, **20**, 2262–2267.
- 18 F. Fu and L. Hu, *Advanced High Strength Natural Fibre Composites in Construction*, 2016, pp. 405–423.
- 19 Promotional LC, Thermometer Sticker 9 to 27 °C – Colour Changing, <https://colourchanging.co.uk/products/promotional-thermometer-sticker-9c-to-27c-10mm-by-70mm-adhesive-backed-strip>, (accessed 17 October 2018).
- 20 Raising the IQ of Smart Windows | Berkeley Lab, <https://newscenter.lbl.gov/2013/08/14/raising-the-iq-of-smart-windows/>, (accessed 17 October 2018).
- 21 M. Moirangthem and A. P. H. J. Schenning, *ACS Appl. Mater. Interfaces*, 2018, **10**, 4168–4172.
- 22 H. Chi, Y. J. Liu, F. Wang and C. He, *ACS Appl. Mater. Interfaces*, 2015, **7**, 19882–19886.
- 23 J. Wei, X. Jiao, T. Wang and D. Chen, *ACS Appl. Mater. Interfaces*, 2016, **8**, 29713–29720.
- 24 J. Lee, C. Y. Koh, J. P. Singer, S. Jeon, M. Maldovan, O. Stein and E. L. Thomas, *Adv. Funct. Mater.*, 2014, **26**, 532–569.
- 25 H. Khandelwal, A. P. H. J. Schenning and M. G. Debije, *Adv. Energy Mater.*, 2017, **7**, 1–18.
- 26 M. Hosseini, A. Salam and H. Makhlof, *Industrial Applications for Intelligent Polymers and Coatings*, Springer International Publishing, 2016.
- 27 H. Hu, Q. W. Chen, K. Cheng and J. Tang, *J. Mater. Chem.*, 2012, **22**, 1021–1027.
- 28 G. Isapour and M. Lattuada, *Adv. Mater.*, 2018, **30**, 1707069.
- 29 A. Schenning, G. P. Crawford and D. J. Broer, *Liquid crystal sensors*, CRC Press, 1st edn, 2017.
- 30 L. Nucara, F. Greco and V. Mattoli, *J. Mater. Chem. C*, 2015, **3**, 8449–8467.
- 31 S. Y. Lee, J. Choi, J. Jeong, J. H. Shin and S. Kim, *Adv. Mater.*, 2017, **29**, 1605450.
- 32 M. Wang and Y. Yin, *J. Am. Chem. Soc.*, 2016, **138**, 6315–6323.
- 33 D. J. Mulder, A. P. H. J. Schenning and C. W. M. Bastiaansen, *J. Mater. Chem. C*, 2014, **2**, 6695.
- 34 Y. Fang, S. Y. Leo, Y. Ni, L. Yu, P. Qi, B. Wang, V. Basile, C. Taylor and P. Jiang, *Adv. Opt. Mater.*, 2015, **3**, 1509–1516.
- 35 D. J. D. Davies, A. R. Vaccaro, S. M. Morris, N. Herzer, A. P. H. J. Schenning and C. W. M. Bastiaansen, *Adv. Funct. Mater.*, 2013, **23**, 2723–2727.
- 36 M. Moirangthem, T. A. P. Engels, J. Murphy, C. W. M. Bastiaansen and A. P. H. J. Schenning, *ACS Appl. Mater. Interfaces*, 2017, **9**, 32161–32167.
- 37 M. Moirangthem, J. E. Stumpel, B. Alp, P. Teunissen, C. W. M. Bastiaansen and A. P. H. J. Schenning, *Proc. SPIE*, 2016, **9769**, 97690Y.
- 38 J. M. Weissman, H. B. Sunkara, A. S. Tse and S. A. Asher, *Science*, 1996, **274**, 959–960.
- 39 M. Kumoda, M. Watanabe and Y. Takeoka, *Langmuir*, 2006, **22**, 4403–4407.
- 40 J. D. Debord and L. A. Lyon, *J. Phys. Chem. B*, 2000, **104**, 6327–6331.
- 41 Z. Hu, X. Lu and J. Gao, *Adv. Mater.*, 2001, **13**, 1708–1712.
- 42 M. Chen, L. Zhou, Y. Guan and Y. Zhang, *Angew. Chem., Int. Ed.*, 2013, **52**, 9961–9965.
- 43 Y. Takeoka and M. Watanabe, *Langmuir*, 2003, **19**, 9104–9106.
- 44 J. H. Kang, J. H. Moon, S. K. Lee, S. G. Park, S. G. Jang, S. Yang and S. M. Yang, *Adv. Mater.*, 2008, **20**, 3061–3065.
- 45 M. C. Chiappelli and R. C. Hayward, *Adv. Mater.*, 2012, **24**, 6100–6104.
- 46 C. Liu, C. Yao, Y. Zhu, J. Ren and L. Ge, *Sens. Actuators, B*, 2015, **220**, 227–232.
- 47 S. J. Jeon, M. C. Chiappelli and R. C. Hayward, *Adv. Funct. Mater.*, 2016, **26**, 722–728.
- 48 Z. Wang, J. Zhang, J. Xie, Z. Wang, Y. Yin, J. Li, Y. Li, S. Liang, L. Zhang, L. Cui, H. Zhang and B. Yang, *J. Mater. Chem.*, 2012, **22**, 7887–7893.
- 49 Y. F. Yue, M. A. Haque, T. Kurokawa, T. Nakajima and J. P. Gong, *Adv. Mater.*, 2013, **25**, 3106–3110.
- 50 S. Valkama, H. Kosonen, J. Ruokolainen, T. Haatainen, M. Torkkeli, R. Serimaa, G. Ten Brinke and O. Ikkala, *Nat. Mater.*, 2004, **3**, 872–876.
- 51 A. J. J. Kragt, D. J. Broer and A. P. H. J. Schenning, *Adv. Funct. Mater.*, 2018, **23**, 1704756.
- 52 H.-S. Kitzerow and C. Bahr, *Chirality in liquid crystals*, Springer-Verlag, New York, 2001.
- 53 J.-W. Wang and B.-Y. Zhang, *Liq. Cryst.*, 2013, **40**, 1550–1560.





- 54 W. Zhang, S. Kragt, A. P. H. J. Schenning, L. T. De Haan and G. Zhou, *ACS Omega*, 2017, **2**, 3475–3482.
- 55 P. Zhang, A. J. J. Kragt, A. P. H. J. Schenning, L. T. De Haan and G. Zhou, *J. Mater. Chem. C*, 2018, **6**, 7184–7187.
- 56 R. Parker, *US Pat.*, 3,861,213, 1975.
- 57 X. Liang, S. Guo, S. Guo, M. Chen, C. Li, Q. Wang, C. Zou, C. Zhang, L. Zhang and H. Yang, *Mater. Horiz.*, 2017, **4**, 878–884.
- 58 X. Liang, C. Guo, M. Chen, S. Guo, L. Zhang, F. Li, S. Guo and H. Yang, *Nanoscale Horiz.*, 2017, **2**, 319–325.
- 59 E. Tian, J. Wang, Y. Zheng, Y. Song, L. Jiang and D. Zhu, *J. Mater. Chem.*, 2008, **18**, 1116–1122.
- 60 H. Yang, L. Pan, Y. Han, L. Ma, Y. Li, H. Xu and J. Zhao, *Appl. Surf. Sci.*, 2017, **423**, 421–425.
- 61 R. A. Barry and P. Wiltzius, *Langmuir*, 2006, **22**, 1369–1374.
- 62 J. H. Kim, J. H. Moon, S.-Y. Lee and J. Park, *Appl. Phys. Lett.*, 2010, **97**, 103701.
- 63 J. Shi, V. K. S. Hsiao, T. R. Walker and T. J. Huang, *Sens. Actuators, B*, 2008, **129**, 391–396.
- 64 E. Kim, S. Y. Kim, G. Jo, S. Kim and M. J. Park, *ACS Appl. Mater. Interfaces*, 2012, **4**, 5179–5187.
- 65 N. Herzer, H. Guneyusu, D. J. D. Davies, D. Yildirim, A. R. Vaccaro, D. J. Broer, C. W. M. Bastiaansen and A. P. H. J. Schenning, *J. Am. Chem. Soc.*, 2012, **134**, 7608–7611.
- 66 J. E. Stumpel, D. J. Broer and A. P. H. J. Schenning, *RSC Adv.*, 2015, **5**, 94650–94653.
- 67 H. Wan, X. Li, L. Zhang, X. Li, P. Liu, Z. Jiang and Z. Z. Yu, *ACS Appl. Mater. Interfaces*, 2018, **10**, 5918–5925.
- 68 K. Yao, Q. Meng, V. Bulone and Q. Zhou, *Adv. Mater.*, 2017, **29**, 1–8.
- 69 R. H. El Halabieh, O. Mermut and C. J. Barrett, *Pure Appl. Chem.*, 2004, **76**, 1445–1465.
- 70 R. Klajn, *Chem. Soc. Rev.*, 2014, **43**, 148–184.
- 71 M. Kamenjicki, I. K. Lednev, A. Mikhonin, R. Kesavamoorthy and S. A. Asher, *Adv. Funct. Mater.*, 2003, **13**, 774–780.
- 72 M. K. Maurer, I. K. Lednev and S. A. Asher, *Adv. Funct. Mater.*, 2005, **15**, 1401–1406.
- 73 K. Matsubara, M. Watanabe and Y. Takeoka, *Angew. Chem., Int. Ed.*, 2007, **46**, 1688–1692.
- 74 S. Kubo, Z.-Z. Gu, K. Takahashi, Y. Ohko, O. Sato and A. Fujishima, *J. Am. Chem. Soc.*, 2002, **124**, 10950–10951.
- 75 S. Kubo, Z. Z. Gu, K. Takahashi, A. Fujishima, H. Segawa and O. Sato, *J. Am. Chem. Soc.*, 2004, **126**, 8314–8319.
- 76 J. Zhao, Y. Liu and Y. Yu, *J. Mater. Chem. C*, 2014, **2**, 10262–10267.
- 77 M. Moritsugu, T. Ishikawa, T. Kawata, T. Ogata, Y. Kuwahara and S. Kurihara, *Macromol. Rapid Commun.*, 2011, **32**, 1546–1550.
- 78 S. Kim, S. Ishii, R. Yagi, Y. Kuwahara, T. Ogata and S. Kurihara, *RSC Adv.*, 2017, **7**, 51978–51985.
- 79 S. Kim, T. Ogata and S. Kurihara, *Polym. J.*, 2017, **49**, 407–412.
- 80 J. C. Hong, J. H. Park, C. Chun and D. Y. Kim, *Adv. Funct. Mater.*, 2007, **17**, 2462–2469.
- 81 H. Yang and P. Jiang, *Langmuir*, 2010, **26**, 13173–13182.
- 82 E. P. A. Van Heeswijk, J. J. H. Kloos, J. De Heer, T. Hoeks, N. Grossiord and A. P. H. J. Schenning, *ACS Appl. Mater. Interfaces*, 2018, **10**, 30008–30013.
- 83 P. M. Resende, R. Sanz, O. Caballero-Calero and M. Martín-González, *Adv. Opt. Mater.*, 2018, **6**, 1800408.

